Reaction Kinetics, Mechanisms and Catalysis (2022) 135:999–1010
https://doi.org/10.1007/s11144-022-02185-y

Green synthesis of palladium nanoparticles and investigation of their catalytic activity for methylene blue, methyl orange and rhodamine B degradation by sodium borohydride

Muradiye Sahin[1] · **Ilkay Hilal Gubbuk**[2]

Received: 12 November 2021 / Accepted: 6 February 2022 / Published online: 11 February 2022

Abstract

In this work, green synthesis, characterization and catalysis applications of antioxidant palladium nanoparticles has been studied in detail. PdNPs was successfully synthesized by using carob, cinnamon, turmeric and ginger antioxidant extracts with green method. Nanoparticles synthesized in this way was characterized by FTIR, UV–Vis, SEM–EDX, TEM and XRD. The UV–Vis spectra of the PdNPs revealed a characteristic surface plasmon resonance peak at 430–435 nm. The synthesized PdNPs reacted as a catalyst to the reduction of dyes (rhodamine B, methyl orange and methylene blue) with $NaBH_4$ (sodium borohydride). Green synthesized antioxidant PdNPs effectively degraded the dyes approximately in 15–22 min and kinetic parameters has been calculated.

✉ Ilkay Hilal Gubbuk
ihilalg@gmail.com

[1] Kırşehir Ahi Evran University, Campus, 40100 Kırşehir, Turkey

[2] Department of Chemistry, Selcuk University, Campus, 42075 Konya, Turkey

Graphical abstract

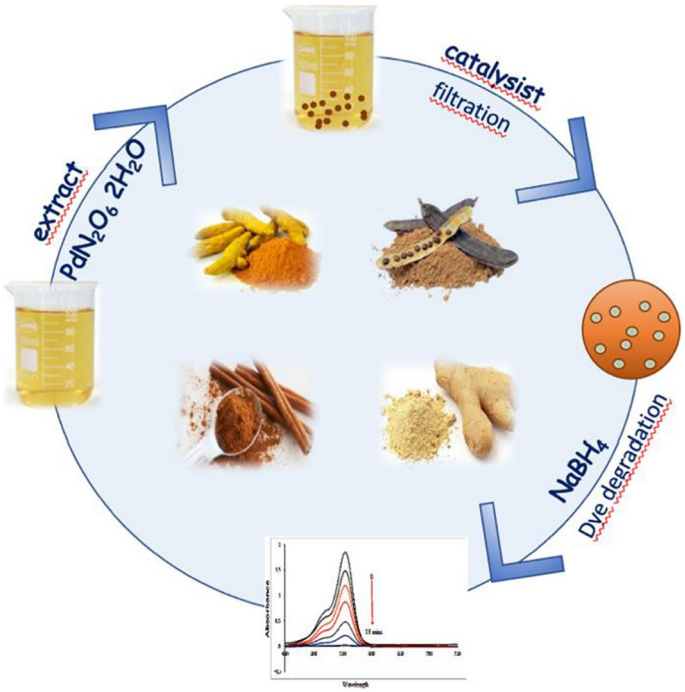

Keywords Antioxidant · Catalytic activity · Dyes · Green synthesis · Nanoparticles

Introduction

Recently metal nanoparticles (MNPs) have been used extensively in the areas alike catalysis, optoelectronics, chemical or biochemical sensors and medicine due to their superior electronics and optical properties [1–5]. There are various physical and chemical available method of preparing MNPs as a catalyst. Despite the successful synthesis of chemical and physical techniques, the interest in cheap and environmentally friendly techniques is increasing due to the environmental and biological harm of the chemicals used. Green Synthesis is economical, does not contain harmful chemicals and it is environment friendly [6–10]. One of the metal nanoparticles are those that contain noble metals. Despite the high materials cost of noble metals, cost effective nano catalyst of this class metals can be prepared using chemical or green synthesis method. Palladium (Pd) is noble metal and is one of the active elements that interact with the surface of oxides as support. In the present work an inexpensive Pd nanoparticle catalyst was prepared using the green method of synthesis with antioxidant extract as a reducing agent. These expensive materials have been made more economical since their surface areas in nanoparticles have increased.

Pd is an important transition metal with high catalytic activity and has diverse applications (oxidation, reduction, Heck reaction, Suzuki coupling e.g.) in the field of both heterogeneous and homogeneous catalyst [11, 12]. Pd is an expensive element, but the synthesis of Pd nanoparticles is cost effective as it reduces the amount of use [13]. Pd metal is one of the most active elements that react with the oxide surface as a support material, so its cost is considered secondary for catalysis studies, especially in which very small amounts are used.

Textile, leather, paper, food, plastic and other industrial waste dyes are the main cause of water pollution [1, 14, 15] most of which are poisonous to plants, animals and humans owing to not being decomposable [1, 16]. Dyes such as methyl orange often threats the environment in terms of mutagenic, carcinogenic and toxic [17]. Therefore it is very important to ensure the degradation of the dyes. PdNPs catalysts always have better selectivity, activity, reaction speed, cost effectiveness, recycling and it provides catalyst / product separation facility [18–21].

The aim of this study is to synthesize noble metal containing nanoparticles (PdNPs) to remove the dyes from watery solution. Antioxidants extracted from the plants prevents oxidation of the particles and gives anti-bacterial properties to the particles [18–22]. Thus, the newly synthesized PdNPs not only remove dyes from the industrial waste water but also prevent possible growth of bacteria in water. In typical reaction instead of using two different agents such as reductant and stabilizer, served as in both a novel material. In addition, water was used as a solvent instead of organic solvents in nanoparticle synthesis. In this research work, three type dyes, methylene blue (a thiazine dye, MB) rhodamine B (an alkaline dye, RB) and methyl orange (an azo dye, MO) with different chemical structures have been chosen to evaluate and compare catalytic performance of as-synthesized materials. Degradation rate of dyes was occurred 100% within 15–22 min. Finally, in this study, it has proved that green synthesized PdNPs have catalytic activity in comprehensive reduction of organic dye compound and high efficiency of Pd.

Material and methods

Materials

Palladium(II) nitrate dihydrate ($N_2O_6Pd.2H_2O$), sodium borohydride ($NaBH_4$) and rhodamine B were received from Sigma Aldrich. Methylene blue was received from Alfa Aesar and methyl orange was received from Merck. Carob, cinnamon, ginger and turmeric powder were purchased from the haberdasher. Double distilled water was used throughout the researches (18.2MΩ). All of the materials were pure and utilized as received without any purification.

Instrumentation

The chemical and morphological characterizations for the nanoparticles were realized by Shimadzu UV-1800 (UV–Vis), Perkin Elmer 100 ATR FT-IR, Carl Zeiss

EVO-LS 10 scanning electron microscope (SEM), JEOL JEM-2100 Transmission Electron Microscope (TEM) and Bruker D8 Advance X-ray diffraction (XRD) with a Cu K_α radiation source in 2θ range from 10° to 80°.

Synthesis of PdNPs

To obtain extracts, 1 g of each plant (carob, cinnamon, ginger and turmeric powder) was gauged and added to 50 mL of distilled water. The mixture was stirred continuously at 25 °C for 5 h at room temperature and was separated by a paper filter [23, 24]. For the preparation of the nanoparticle with Pd, the each extract (7 mL) was added to 0.01 M (133 mg) 50 mL of $Pd(NO_3)_2.2H_2O$. Solutions were left at room temperature under magnetically stirring for completion of the synthesis. Plant extracts acted as reductants for the reduction of Pd ions. After the reduction of ions (Pd^{2+}) to Pd (Pd^0) was completed for about 15–20 min, the nanoparticles were filtered through a Whatman No 1 filter paper (90 mm, 82 g/m^2 and pore size: 15–19 µm). The formation of nanoparticles was also recognized by the color change and observed by UV–Vis spectrum analysis (Fig. S1) [25, 26]. As a result, 98 mg PdNPs were synthesized in high yield (81.66%) in an environmentally friendly method using the antioxidant extract of carob, cinnamon, ginger and turmeric powder at room temperature without using any reducing chemicals.

Catalytic activity of PdNPs

The catalytic activity of PdNPs were studied using the degradation of dyes such as rhodamine B, methylene blue and methyl orange using $NaBH_4$. These three dyes are chosen in this research, due to the exhibition of distinct colors in the reduced and oxidized structures, and not to overlap the SPR band of PdNPs with their absorption peak. The reduction of MO, RB and MB by $NaBH_4$ in the existence of each PdNPs as a heterogen catalyst at 25 °C was conducted. 1 mL of $NaBH_4$ (1×10^{-2} mol L^{-1}) is mixed with 1 mL of dye solution (1×10^{-5} mg L^{-1}), 0.5 mL Pd (9 mg) nanoparticles were added to this mixture and then the UV–Vis spectra have been registered at orderly intervals of time (Fig. S2). Reduction of all dyes are shown by the decolorization of the solution to colorless. Concentrations of RB, MO and MB dyes were quantified by measuring the absorption band at 554, 460 and 664 nm.

Results and discussion

Characterization

The PdNPs were characterized by FTIR, UV–Vis, HR-TEM (high resolution-TEM), XRD and SEM–EDX. The UV–Vis suction spectroscopy is a generally used practice to qualify different metal nanoparticles [27]. Synthesis of PdNPs using antioxidant extracts were firstly reputed with the color changes. A light brown color of watery solution gradually changed to black color for all nanoparticles. By the UV–Vis

spectral analysis, the characteristic absorbance peak at 430–435 nm is commonly used for the definition of PdNPs [28]. Fig. S2 shows the each of the characteristic absorbance peak at this wavelength of the PdNPs [18].

Comparative FTIR spectra of plants and PdNPs containing these plants are shown in Fig. S3. FTIR analysis of four plants (carob, cinnamon, turmeric and ginger) includes chemical structures containing amine, alkali, methylene, alkene and carboxyl groups. These chemical groups are known to be reducing agents that aid in the synthesis of nanoparticles [29]. In the FTIR spectra of plants, peaks are seen at approximately 710 cm^{-1}, 1650 cm^{-1}, 1766 cm^{-1}, 2961 cm^{-1} and 3274 cm^{-1}. The peak at 3274 cm^{-1} is due to –OH groups stretching vibration. Peak at 2961 cm^{-1} is because of N–H bond, 1766 cm^{-1} (C=C double bonds or aromatic rings) and 1650 cm^{-1} (C=O groups of carboxylic acids and –NH bond stretching of amide linkages). The comparison of plant and nanoparticle spectra shows that 1650 cm^{-1} wavenumber the peak intensity decreases and absorption at 1500 cm^{-1} the band has been shown to strengthen, which leads to the formation of Pd nanoparticles [30]. FTIR spectra of plant containing PdNPs show a significant shift in hydroxyl, carbonyl and amino group bands. This is due to the reduction of PdNPs, the interaction of existing hydroxyl and carbonyl groups and it shows the involvement of -COOH group in the synthesis of nanoparticles [31].

XRD analyzes were conducted to determine the crystal structure of the obtained Pd nanoparticles. XRD results of synthesized PdNPs is given in Fig. S4. The XRD study of the PdNPs showed that four diffraction peaks at 2-Theta (2θ) values of 38.1°, 44.8°, 63.8° and 73.8° correspond to the diffraction from (111), (200), (220) and (311), which can be indexed to crystallographic planes of (face centered cubic) fcc Pd nanoparticles. XRD results are compatible with (Joint committee on powder diffraction standards) JCPDS 89-4897 PDF file [32]. The crystal size is calculated for each PdNPs by applying the Scherrer equation (Eq. 1) due to strongest (111) reflection of plane. The average crystal size is 15.4 nm, 16 nm, 15 nm and 14 nm for carob, cinnamon, turmeric and ginger antioxidant nanoparticle.

$$D_{111} = \frac{k\lambda}{\beta \cos\theta} \tag{1}$$

Here D is crystallite size, k (0.891) is Debye–Scherrer's constant, λ (1.5406 Å) stands for X-ray wavelength, β indicates the full width at half maximum intensity (*FWHM*) of the XRD peaks and θ is the diffraction angle (2θ).

The shape and size of the PdNPs were additionally characterized by TEM and SEM analysis. The exemplary TEM and SEM images of PdNPs at distinct magnifications are submitted in Figs. S5 and S6. The SEM images show individualistic PdNPs besides a series of aggregates. Fig. S5 obviously indicates the presence of the synthesized Pd nanoparticles with magnification × 10,000 and × 20,000. Generally, nanoparticles were oval, spherical in shape and aggregated. Fig. S5 indicates the EDX spectra of PdNPs synthesized at room temperature to confirm even stronger the entity of Pd atoms in PdNPs. Entity of the elemental Pd can be observed in the graph attained from EDX analysis. The optic absorption peak was monitored at 3.2 keV, 3.0 keV, 2.8 keV and 2.6 keV, which is characteristic for the absorption of PdNPs due to SPR. In this way,

this standed that the elements obtained was a Pd. Further, EDX analysis showed low signals of magnesium, oxygen and iron.

From TEM images obviously shows that the nanoparticles are nearly spherical in shape. Fig. S6 also indicates that the size distribution histogram of the particles, the mean size of the particles is found to be 22.56 ± 0.20 nm and the size of the nanoparticles varies amongst 10 nm and 35 nm. HR-TEM analysis indicates sharp lattice eaves (Fig. S6). SAED (selected area electron diffraction) model approves the crystal structure of the nanoparticles. The brilliant circular dots observed in the electron diffraction pattern conformed to (111), (200), (220) and (311) reflexion surfaces. PdNPs were polycrystalline, and as could be seen from the SAED, all the PdNPs have single orientation figuration such as a cluster of Pd particles. In this way, synthesized PdNPs are extremely crystalline as shown by HR-TEM and SAED.

Catalytic activity

MB, MO and RB dyes were each reduced at 25 °C with PdNP containing four types of antioxidants. This process is above which was made as described in Section "Catalytic activity of PdNPs" and Fig. S2. These dyes and their degradation products are given in Fig. S7. In this study, Pd nanoparticles synthesized by the green method were used to remove dyes by chemical catalysis in the presence of $NaBH_4$. Firstly, dye degradation studies were performed without using PdNPs. For the degradation study, 1 mL of dye was taken in quartz cuvettes; to this solution was added 1.5 mL of $NaBH_4$ (1×10^{-2} mol L^{-1}) solution. First there was some color change in the dyes to the light form afterwards $NaBH_4$ could not further reduce the dye even after 1 to 2 h. Without NPs, $NaBH_4$ is not that effective in fully reducing the dye. Metals such as Pd are needed to completely reduce the dye compound to the degradation product. As a dye degradation reaction, it has been suggested that $NaBH_4$ is decomposed into BH_4^- by PdNPs and subsequently produces ***H–Pd*** and Pd-BH_3^- as reactive intermediates. The ***Pd–H*** reagent is responsible for converting the dye into a harmless degradation product for all dye types [33].

$$2Pd + BH_4^- \leftrightarrow Pd{-}BH_3^- + \mathbf{Pd{-}H}$$

$$\mathbf{H{-}Pd} + PdNPs \rightarrow Pd{-}\mathrm{Dye} + Pd + H$$

$$Pd{-}BH_3 + PdNPs \rightarrow Pd{-}\mathrm{Dye} + Pd + BH_3$$

Similarly, in the work by Vidhu and Philip, Ag doped catalyst was used and a similar catalysis mechanism was formed. It is accepted that the possible degradation reaction mechanism of the dyes occurs through the following steps [34].

$$\mathrm{Ag/NaBH_4} + \mathrm{h}\surd \rightarrow \mathrm{Ag/NaBH_4}\left(\mathrm{h^+{-}e^-}\right)$$

$$2\mathrm{e^-} + \mathrm{MOH^+} + \mathrm{H^+} \rightarrow \mathrm{MOH_2^-(degradation\ products)}$$

Kinetic study

The process of catalytic degradation of MB, MO and RB were found to follow the pseudo-first-order kinetic model.

$$-\frac{dc_t}{dt} = kc \tag{2}$$

$$\frac{c}{c_0} = Ae^{-kt} + E \tag{3}$$

Here C and C_0 are dyes concentrations at time t and 0. k is the reaction rate constant; t is the reaction time. The values of rate constant and standard deviations are obtained by non-linear least squares fitting [35, 36], as shown in Figs. 1a, 2a, 3a and Table 1.

$$t_{1/2} = ln2/k \tag{4}$$

Equation 4 can be used to calculate the half-life $t_{1/2}$ of dyes with various PdNPs and all results are listed in Table 1. Moreover, the catalytic degradation is calculated according to Michaelis–Menten kinetics [36] and the effect of the initial concentration on the degradation rate is found by the Eq. 5.

$$V = \frac{V_{max}C}{K_M + C} \tag{5}$$

Here, v is the initial rate, c represents concentration, v_{max} and K_M are related to maximum initial rate and Michaelis constant. When the initial concentration

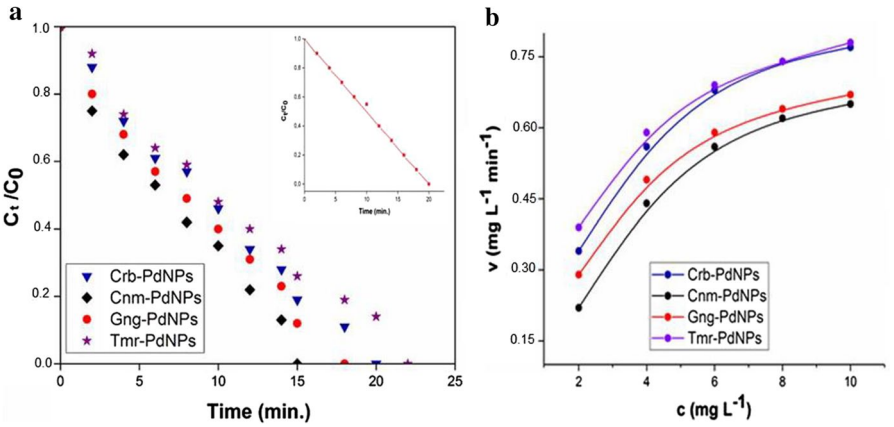

Fig. 1 **a** Pseudo-first order kinetic model for degradation of MB, **b** The curves of the Michaelis–Menten kinetics of the degradation of MB by four type PdNPs. The above curves were obtained by non-linear least squares fitting. (Concentration of MB; 1 mL, 1×10^{-5} mg L^{-1}, $NaBH_4$; 1 mL 1×10^{-2} mol L^{-1}, each of nanoparticle solution with water; 0.5 mL)

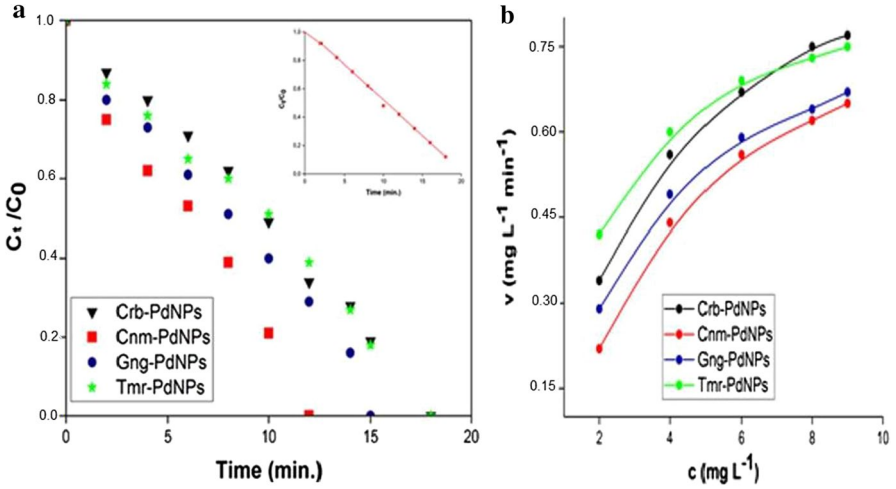

Fig. 2 **a** Pseudo-first order kinetic model for degradation of MO, **b** The curves of the Michaelis–Menten kinetics of the degradation of MO by four type PdNPs. The above curves were obtained by non-linear least squares fitting. (Concentration of MO; 1 mL, 1×10^{-5} mg L^{-1}, $NaBH_4$; 1 mL 1×10^{-2} mol L^{-1}, each of nanoparticle solution with water; 0.5 mL)

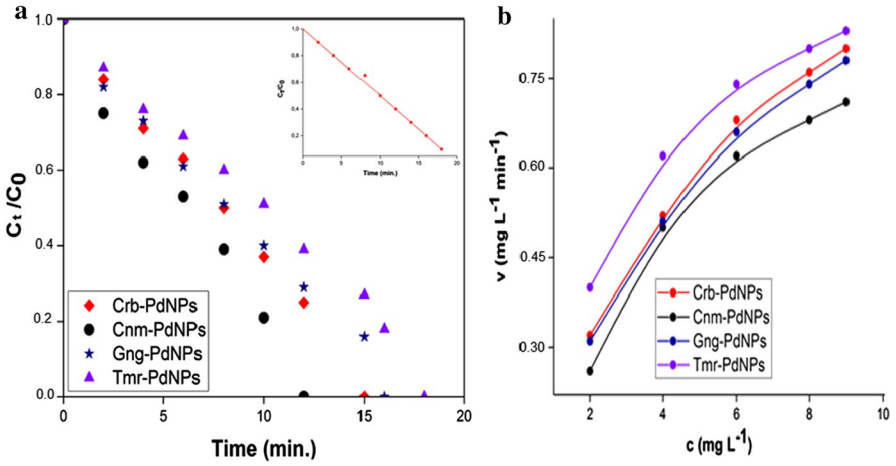

Fig. 3 **a** Pseudo-first order kinetic model for degradation of RB, **b** The curves of the Michaelis–Menten kinetics of the degradation of RB by four type PdNPs. The above curves were obtained by non-linear least squares fitting. (Concentration of RB; 1 mL, 1×10^{-5} mg L^{-1}, $NaBH_4$; 1 mL 1×10^{-2} mol L^{-1}, each of nanoparticle solution with water; 0.5 mL)

range of MB, MO and RB are 2–10 mg L^{-1}, the values of v_{max} and K_M can be obtained by non-linear least squares fitting [37]. Figures 1b, 2b, 3b depict that the dye concentration range in Michaelis–Menten curve is suitable. v_{max} and K_M are calculated as 0.7856 ± 0.0098 mg L^{-1} min^{-1} and 3.1920 ± 0.098 mg L^{-1}.

Table 1 Kinetic data of the nanoparticles

Dye	PdNPs samples	k (min^{-1})	R^2	$t_{1/2}$ (min)
MB	Crb-PdNPs	0.0699	0.9820	9.92
	Cnm-PdNPs	0.0912	0.9917	7.60
	Gng-PdNPs	0.0820	0.9901	8.45
	Tmr-PdNPs	0.0651	0.9558	10.65
MO	Crb-PdNPs	0.0814	0.9799	8.52
	Cnm-PdNPs	0.1326	0.9917	5.23
	Gng-PdNPs	0.1041	0.9708	6.66
	Tmr-PdNPs	0.0817	0.9877	8.48
RB	Crb-PdNPs	0.1051	0.9877	6.60
	Cnm-PdNPs	0.1273	0.9930	5.45
	Gng-PdNPs	0.0908	0.9804	7.63
	Tmr-PdNPs	0.0836	0.9692	8.29

MB is found to have numerous uses in a large area of including biology and chemistry which is a cationic thiazine dye. MB is used in the analysis of trace grade of sulphuret ions in aquatic sample. The hydrated solution of the oxidate structure of MB is deep blue in color and leuco form (its reduced form) is uncolored. Fig. S8 and Fig. 1a indicates the UV–Vis spectrum registered at 2 min intervals for the degradation of MB catalyzed by PdNPs at room temperature.

MO which is frequently used as an indicator in diverse analytical areas, is an organic azo dye. Reduction of multicolored MO is an amazing field of study owing to pollution problems it possess. The aqueous solution of MO is orange in color. The UV–Vis spectrum of aqueous solution of MO indicates robust absorptions at 460 nm. The UV–Vis absorption spectra listed during the degradation of MO by $NaBH_4$ in entity of PdNPs catalyst at room temperature and resulted seen in Fig. S9 and Fig. 1b.

RB is a fluorescent dye associated to the family of xanthenes. RB dyes are greatly used as fluorescent probes due to wide fluorescence in the visible field of electromagnetic spectrum and their superior absorption factor. Their perfect physical properties enables to be used in textile industry and creates a major dye pollutant. The aqueous solution of RB is pink in color. The UV–Vis absorption spectrum listed during the degradation of RB by $NaBH_4$ in entity of PdNPs catalyst at room temperature and resulted seen in Fig. S10 and Fig. 1c.

To show the advantage of the antioxidant PdNPs over some of the reported catalysts in the literature, the catalytic role of the different plant extract using synthesized PdNPs in the degradation of dyes with $NaBH_4$ was compared with various reported catalyst (Table 2). The results show that in comparison with other catalysts, the antioxidant PdNPs is the most efficient catalyst with respect to the reaction time, which is probably attributed to the presence of the PdNPs with small sizes.

Table 2 A comparison between the catalytic activity loading for different plant extract mediated synthesized NPs and their degradation of dyes

Dye	Time (min)	References
Methyl Orange	140 min	[17]
	30 min	[38]
	12–18 min	Present work
Methylene Blue	40 min	[17]
	40 min	[16]
	30 min	[14]
	15–22 min	Present work
Rhodamine B	90 min	[17]
	40 min	[14]
	12–18 min	Present work

Conclusion

Antioxidant PdNPs were prepared successfully via a facile, simple, economic, and eco-friendly route from carob, cinnamon, turmeric and ginger extracts. The UV–Vis, FTIR, SEM–EDX, TEM and XRD analysis results approved the genesis of nanoparticles. The catalytic feature of the Crb-PdNPs, Cnm-PdNPs, Gng-PdNPs and Trm-PdNPs in degrading RB, MB and MO to their end products in the presence of $NaBH_4$ at room temperature were studied. Antioxidant PdNPs in the existence of $NaBH_4$ catalyze the degradation reaction, which leads to the removal of RB, MB and MO. Absorbance became almost zero in all of dyes. Thus Crb-PdNPs, Cnm-PdNPs, Gng-PdNPs and Trm-PdNPs provided a good electron transfer that catalyzes the reactions by reducing the activation energy. Also, as a reducing agent, $NaBH_4$, was not capable to reduce RB, MB and MO in absence of a catalyst, indicating the efficacy of Crb-PdNPs, Cnm-PdNPs, Gng-PdNPs and Trm-PdNPs. Therefore, it was concluded that antioxidant PdNPs significantly reduce the color of MO, RB and MB dyes in the existence of $NaBH_4$. Comprehensively in addition, the same catalyst was also used in the degradation of hazardous dyes and Pd is considered to be a metal with effective catalytic properties.

Supplementary Information The online version contains supplementary material available at https://doi.org/10.1007/s11144-022-02185-y.

Acknowledgements This work was supported by a grant of Selcuk University Research Coordination Office, Konya, Turkey, for the project 19201061.

References

1. Jaleh, B., Karami, S., Sajjadi, M., Mohazzab, B.F., Azizian, S., Nasrollahzadeh, M., Varma, (2020) Laser-Assisted Preparation of Pd Nanoparticles on Carbon Cloth for the Degradation of Environmental Pollutants in Aqueous Medium. Chemosphere, 246: 125755.

2. Blosi M, Albonetti S, Ortelli S, Costa A, Ortolani L, Dondi M (2014) Green and easily scalable microwave synthesis of noble metal nanosols (Au, Ag, Cu, Pd) usable as catalysts. New J Chem 38(4):1401–1409
3. Dinh N, Leopold M, Coppage R (2018) Sintering-induced nucleation and growth of noble metal nanoparticles for plasmonic resonance ceramic color. J Inorg Organomet Polym Mater 28:2770–2778
4. Nadagouda MN, Iyanna N, Lalley J, Han C, Dionysios DD, Varma RS (2014) Synthesis of silver and gold nanoparticles using antioxidants from blackberry, blueberry, pomegranate and turmeric extracts. ACS Sust Chem Eng 2:1717–1723
5. Deepika H, Jacob L, Mallikarjuna NN, Rajender SV (2013) Greener techniques for the synthesis of silver nanoparticles using plant extracts, enzymes, bacteria, biodegradable polymers, and microwaves. ACS Sust Chem Eng 1(7):703–712
6. Alsammarraie FK, Wang W, Zhou P, Mustapha A, Lin M (2018) Green synthesis of silver nanoparticles using turmeric extracts and investigation of their antibacterial activities. Colloids Surf, B 171:398–405
7. Arya G, Kumari RM, Gupta N, Kumar A, Chandra RN, S, (2018) Green synthesis of silver nanoparticles using Prosopis juliflora bark extract: reaction optimization, antimicrobial and catalytic activities. Art Cells Nanomed Biotechnol 46(5):985–993
8. Bogireddy NKR, Pal U, Gomez LM, Agarwal V (2018) Size controlled green synthesis of gold nanoparticles using Coffea arabica seed extract and their catalytic performance in 4-nitrophenol reduction. RSC Adv 8:24819–24826
9. Kou J, Varma RS (2012) Beet juice utilization: Expeditious green synthesis of noble metal nanoparticles (Ag, Au, Pt, and Pd) using microwaves. RSC Adv 2(27):10283–10290
10. Makarov VV, Love AJ, Sinitsyna OV, Makarova SS, Yaminsky IV, Taliansky ME, Kalinina NO (2014) Green nanotechnologies: synthesis of metal nanoparticles using plants. Acta Nat 6(1):35–44
11. Sa S, Gawande MB, Velhinho A, Veiga JP, Bundaleski N, Trigueiro J, Tolstogouzov A, Teodoro OMND, Zboril R, Varma RS, Branco S (2014) Magnetically recyclable magnetite–palladium (Nanocat-Fe–Pd) nanocatalyst for the Buchwald-Hartwig reaction. Green Chem 7(16):3494–3500
12. Corma A, Garcia H, Leyva A (2005) Catalytic activity of palladium supported on single wall carbon nanotubes compared to palladium supported on activated carbon: study of the Heck and Suzuki couplings, aerobic alcohol oxidation and selective hydrogenation. J Mol Catal A Chem 230:97–105
13. Baruah D, Das RN, Hazarika S, Konwar D (2015) Biogenic synthesis of cellulose supported Pd(0) nanoparticles using hearth wood extract of Artocarpus lakoocha Roxb- A green, efficient and versatile catalyst for Suzuki and Heck coupling in water undermicrowave heating. Catal Commun 72:73–80
14. Khodadadi B, Bordbar M, Nasrollahzadeh M (2017) Achillea millefolium L. Extract mediated green synthesis of waste peach kernel shell supported silver nanoparticles: application of the nanoparticles for catalytic reduction of a variety of dyes in water. J Colloid Interface Sci 493:85–93
15. Varma RS (2012) Greener approach to nanomaterials and their sustainable applications. Curr Opin Chem Eng 1:123–128
16. Mata R, Bhaskaran A, Sadras SR (2016) Green-synthesized gold nanoparticles from Plumeria alba flowerextract to augment catalytic degradation of organic dyes and inhibitbacterial growth. Particuology 24:78–86
17. Salehi MH, Yousefi M, Hekmati M, Balali E (2019) In situ biosynthesis of palladium nanoparticles on Artemisia abrotanum extract-modified graphene oxide and its catalytic activity for Suzuki coupling reactions. Polyhedron 165:132–137
18. Kora AJ, Rastogi L (2018) Green synthesis of palladium nanoparticles using gum ghatti (Anogeissus latifolia) and its application as an antioxidant and catalyst. Arab J Chem 11:1097–1106
19. Selim A, Kaur S, Dar AH, Sartaliya S, Jayamurugan G (2020) Synergistic effects of carbon dots and palladium nanoparticles enhance the sonocatalytic performance for rhodamine B degradation in the absence of light. ACS Omega 5:22603–22613
20. Omidvar A, Jaleh B, Nasrollahzadeh M (2017) Preparation of the GO/Pd nanocomposite and its application for the degradation of organic dyes in water. J Colloid Interface Sci 496:44–50
21. Chen A, Ostrom C (2015) Palladium-based nanomaterials: synthesis and electrochemical applications. Chem Rev 115:11999–12044
22. Seku K, Gangapuram BR, Pejjai B, Kadimpati KK, Golla N (2018) Microwave-assisted synthesis of silver nanoparticles and their application in catalytic, antibacterial and antioxidant activities. J Nanostruct Chem 8:179–188

23. Sahin M, Gubbuk IH (2019) Green synthesis of antioxidant silver and platinum nanoparticles using ginger and turmeric extracts and investigation of their catalytic activity. J Turkish Chem Soc A 6(3):403–410
24. Han Z, Dong L, Zhang J, Cui T, Chen S, Ma G, Guoa X, Wang L (2019) Green synthesis of palladium nanoparticles using lentinan for catalytic activity and biological applications. RSC Adv 9:38265–38270
25. Nasrollahzadeha M, Sajadib SM, Maham M (2015) Green synthesis of palladium nanoparticles using Hippophaerhamnoides Linn leaf extract and their catalytic activity for theSuzuki–Miyaura coupling in water. J Mol Catal A: Chem 396:297–303
26. Shaik MR, Ali ZJQ, Khan M, Kuniyil M, Assal ME, Alkhathlan HZ, Al-Warthan A, Siddiqui MRH, Khan M, Adil SF (2017) Green synthesis and characterization of palladium nanoparticles using origanum vulgare L extract and their catalytic activity. Molecules 22:165–177
27. Baruwati B, Varma RS (2009) High value products from waste: grape pomace extract—a three-in-one package for the synthesis of metal nanoparticles. Chem Sus Chem 2(11):1041–1044
28. Borodko Y, Lee HS, Joo SH, Zhang Y, Somorjai G (2010) Spectroscopic study of the thermal degradation of PVP-capped Rh and Pt Nanoparticles in H_2 and O_2 environments. J Phys Chem C 114:1117–1126
29. Sathishkumar M, Sneha K, Kwak IS, Mao J, Tripathy SJ, Yun YS (2009) Phyto-crystallization of palladium through reduction process using *Cinnamom zeylanicum* bark extract. J Hazard Mater 171:400–404
30. Amrutham S, Maragoni V, Guttena V (2020) One-step green synthesis of palladium nanoparticles using neem gum (Azadirachta Indica): characterization, reduction of Rhodamine 6G dye and free radical scavenging activity. Appl Nanosci 10:4505–4511
31. Lebaschi S, Hekmati M, Veisi H (2017) Green synthesis of palladium nanoparticles mediated by black tea leaves (Camellia sinensis) extract: Catalytic activity in the reduction of 4-nitrophenol and Suzuki-Miyaura coupling reaction under ligand-free conditions. J Colloid Interface Sci 485:223–231
32. Ngnie G, Dedzo GK, Detellier C (2016) Synthesis and catalytic application of palladium nanoparticles supported on kaolinite-based nanohybrid materials. Dalton Trans 45(22):9065–9072
33. Anjum F, Gul S, Khan MI, Khan MA (2020) Efficient synthesis of palladium nanoparticles using guar gum as stabilizer and their applications as catalyst in reduction reactions and degradation of azo dyes. Green Process Synth 9:63–76
34. Vidhu VK, Philip D (2014) Catalytic degradation of organic dyes using biosynthesized silver nanoparticles. Micron 56:54–62
35. Xu Q, Mavengere S, Kim JS (2021) Preparation of the $CaAl_2O_4$:Eu^{2+}, Nd^{3+}/TiO_2 composite by peroxo titanium complex solution and its photodegradation of methylene blue. React Kinet Mech Catal 134:473–484
36. Lente G (2018) Facts and alternative facts in chemical kinetics: remarks about the kinetic use of activities, termolecular processes, and linearization techniques. Curr Opin Chem Eng 21:76–83
37. Gholami P, Dinpazhoh L, Khataee A, Hassani A, Bhatnagar A (2020) Facile hydrothermal synthesis of novel Fe-Cu layered double hydroxide/biochar nanocomposite with enhanced sonocatalytic activity for degradation of cefazolin sodium. Journal of Hazardous Materials, 381:120742
38. Sreekanth TVM, Jung MJ, Eom IY (2016) Green synthesis of silver nanoparticles, decorated on graphene oxide nanosheets and their catalytic activity. Appl Surf Sci 361:102–106